Melting of a quasi-two-dimensional metallic system

Dmitriy S. Chekmarev, David W. Oxtoby, and Stuart A. Rice
Department of Chemistry and The James Franck Institute, The University of Chicago, Chicago, Illinois 60637
(Received 19 September 2000; revised manuscript received 22 January 2001; published 11 April 2001)

We analyze the melting of a quasi-two-dimensional metallic system using the results of a series of Monte Carlo simulations of an array of Pb atoms. The system was chosen to model the melting behavior observed for the monolayer of Pb that segregates in the liquid-vapor interface of a dilute Pb in Ga alloy [B. Yang *et al.*, Proc. Natl. Acad. Sci. USA **96**, 13 009 (1999)]. Our calculations employed a realistic pair interaction potential between lead pseudoatoms, one that is known to describe accurately the properties of the three-dimensional metal near the melting point. Our results reveal that in the quasi-two-dimensional Pb system melting is a two-stage process which proceeds through formation of a stable intermediate hexatic phase, in agreement with the prediction of the Kosterlitz-Thouless-Halperin-Nelson-Young theory. Both the solid-to-hexatic and the hexatic-to-liquid transitions are found to be first order in our simulations.

DOI: 10.1103/PhysRevE.63.051502 PACS number(s): 64.70.Dv, 68.03.−g

I. INTRODUCTION

The work reported in this paper was stimulated by the results of recent x-ray reflectivity and grazing incidence x-ray diffraction studies of the structure of the Pb monolayer that segregates in the liquid-vapor interface of a dilute Pb in Ga alloy [1,2]. That Pb monolayer completely covers the surface of the alloy. When $T<66\,^{\circ}\mathrm{C}$ the Pb atoms in the monolayer form a two-dimensional (2D) hexagonal lattice. At 66 °C the Pb monolayer undergoes a melting transition that is inferred to be first order on the basis of the apparently discontinuous change in the range of the translational order. Since the locations of the peaks in the diffraction patterns of the ordered and disordered phases below and above the transition temperature are the same within the experimental precision, it is inferred that there is a zero (or very small) density change across the transition. As to the substrate, over the entire (limited) temperature range studied the in-plane structure of the Ga and the atomic distribution of Ga along the normal to the interface do not exhibit any significant differences from the corresponding distributions in the liquid-vapor interface of pure Ga.

The results just described are striking. Earlier studies of the structures of the monolayers of Bi, In, and Sn that segregate in the liquid-vapor interfaces of their respective dilute alloys with liquid Ga have led to the conclusion that all of those monolayers are quasi-2D liquids [3]. Moreover, liquid Ga does not provide any pinning potential that might aid in stabilizing an ordered solid phase of the segregated monolayer. It is certainly interesting to determine why the structure of the liquid-vapor interface of a Pb in Ga alloy is so different from the structures of the liquid-vapor interfaces of Bi, In, and Sn in Ga alloys. And, accepting the experimental results, it appears that the Pb in Ga alloy system provides an unusual vehicle with which one can study the structure and phase diagram of a quasi-2D system.

Experimental studies of the structure of the liquid-vapor interface of an alloy are difficult to execute. In the particular case of Pb in Ga, the data available are not sufficient to resolve many important issues. Specifically, the character of the translationally disordered phase is not determined by the available data and the inferred character of the melting transition needs to be confirmed. The calculations reported in this paper were designed to provide information with which these issues can be resolved.

A segregated monolayer of Pb supported on liquid Ga is a complex many body system. We have adopted the simplest possible model of the Pb monolayer, namely, that it can be treated as an isolated quasi-2D system, neglecting the interactions between the Pb atoms and the supporting Ga substrate. In fact, self-consistent quantum Monte Carlo simulation studies of the liquid-vapor interface of Pb in Ga alloys, by Zhao and Rice [4], yield the result that the effective interaction between the Pb atoms and the substrate Ga is very weak. Nevertheless, because neglect of the Ga substrate also implies neglect of the requirement of equality of chemical potentials of the electrons in the Pb layer and in bulk liquid Ga, our model is a drastic simplification of reality. Accepting that difficulty, we expect that when a reasonable pseudopotential is used the qualitative features of the structure of the 2D assembly of Pb atoms will be properly described. For our calculations we have used a recently reported, uncomplicated, yet powerful, model pseudopotential proposed by Fiolhais *et al.* [5]. This class of pseudopotentials has been proved to provide an accurate description of the structure and thermodynamic properties of bulk crystalline and liquid simple metals.

II. BACKGROUND INFORMATION

The nature of phase transitions in low-dimensional systems remains one of the forefront problems in modern condensed matter physics and chemistry. Consider, for example, crystallization in two dimensions. It is known that at any nonzero temperature a classical 2D solid lacks genuine long range translational order (crystalline order) [6] because thermally induced fluctuations are strong enough to disrupt that order in the thermodynamic limit. In this case the true long range translational order (LRTO) of a crystalline array is replaced by quasi-long-range translational order (QLRTO). The difference between these categories of long range order is in the variation of the envelope of the density-density cor-

relation function in the limit $r \to \infty$: for a LRTO system, e.g., a typical 3D solid, this correlation function decays to a nonzero constant value, whereas for a QLTRO system the decay takes the form of a power law ($r^{-\eta}$). A 2D solid possesses a still different type of long range order, called bond orientational order. When the solid carries this specific type of order, the orientations of virtual bonds that connect two nearest neighbors, as measured in some fixed system of coordinates, are correlated over indefinitely large interparticle separations.

We note in passing that the absence of long range translational order in quantum 2D solids has also been documented [7].

Given such a profound qualitative difference between the structures of 2D and 3D solids, it is not unreasonable to expect that the mechanisms by which these structures are brought about (crystallization) or destroyed (melting) will also differ substantially. The most renowned theoretical framework for 2D melting, the Kosterlitz-Thouless-Halperin-Nelson-Young (KTHNY) formalism, supplies compelling evidence for this expectation. According to the KTHNY theory [8,9], 2D melting is a two-stage process that proceeds through formation of a unique stable intermediate phase known as a *hexatic*. The first transition, which is driven by spontaneous unbinding of the dislocation pairs to produce a ''gas'' of free dislocations, transforms the system from a solid to a hexatic phase. The latter is a translationally disordered phase with quasi-long-range bond orientation order (i.e., there is an algebraic decay of the envelope of the corresponding correlation function in the thermodynamic limit). In the following transformation dislocations dissociate further to form free disclinations, converting the hexatic phase into a fully disordered fluid. The KTHNY theory predicts both transitions to be continuous, albeit it does not stipulate this to be the only possibility. In fact, another representative of a class of defect mediated theories of 2D melting, the Chui theory, proposes a competing scenario according to which the KTHNY sequence can be preempted by grain-boundary-induced melting. The grain boundaries can be thought of as collective excitations of defects. In this case there is a first order solid-to-liquid transition [10].

We remark here that the KTHNY approach to 2D melting identifies the transition with the limit of mechanical stability of the solid. The theory does not include any description of the liquid state and does not address any possible difference between the limit of mechanical stability and the limit of thermodynamic stability which defines the melting point as the temperature (and pressure) at which the chemical potentials of the solid and liquid phases are equal. As formulated, the KTHNY theory can be applied to any system that can be approximated as a continuous elastic medium, regardless of the form of the interparticle potential energy function. The theory focuses attention on locating the points at which a 2D solid becomes unstable with respect to proliferation of certain types of topological defect, and it exploits the consequences of the assumption that the density of topological defects remains small throughout the transition sequence. Glaser and Clark [11] have proposed an alternative interpretation of 2D melting, which they view as a type of defect condensation process. This theory exploits the properties of geometric defects that are thermally induced and localized, in contrast with the topological defects used in the KTHNY formalism. Glaser and Clark concluded that the 2D solid-to-liquid transition is first order, without the occurrence of an intermediate hexatic phase.

In the past two decades numerous tests of the predictions of the KTHNY theory have been reported. The majority of these tests have been based on computer simulation studies, but there have also been a number of tests based on experimental studies of various realizations of a 2D system [12–14]. We will refer to all of the experimental realizations as quasi-two-dimensional, since each must account for the effects of interaction with a supporting substrate or confining walls, and each must assess the importance or lack thereof of motion out of the plane of assembly. The results of these experimental and theoretical studies only partially answer, or leave unanswered, three questions of interest to us: (1) How is a solid-to-liquid phase transition in two dimensions influenced by the form of the interparticle potential energy function? (2) Does this transition in different physical systems follow the same path, as prescribed by the KTHNY theory, or does it follow a system dependent path? (3) What is the domain of stability of the hexatic phase, and does that domain depend on the form of the interaction potential?

An indication that the nature of a solid-to-liquid phase transition in two dimensions may be sensitive to the form of the particle-particle interaction potential has been demonstrated by Bladon and Frenkel [15]. They carried out simulations of a model system composed of hard disks that interact via a pairwise additive potential that includes a hard-core repulsion and a very narrow square-well attraction (or repulsion). This interaction potential supports two high-density 2D ordered solid phases with the same symmetry but different densities. Because the symmetries of the two solid phases are the same, transitions between them define a coexistence line that ends at a critical point. In the vicinity of that critical point there are pronounced density fluctuations, with the consequence that the lower-density solid becomes unstable with respect to dislocation unbinding and the system supports a hexatic phase. When the width of the potential well approaches a limiting value (for this system about 8% of the particle diameter), the domain of stability of the hexatic phase extends to the melting line, so that the overall melting process can be described by the sequence of transitions solid-to-hexatic (either first order or continuous) and hexatic-to-liquid (first order). The behavior predicted by the Bladon-Frenkel simulations has been strikingly confirmed by the results of a series of experiments reported by Marcus and Rice [13], who studied a quasi-2D system of sterically stabilized colloid particles. The interaction between a pair of these particles is qualitatively similar to that assumed in the Bladon and Frenkel simulations; it has a steeply (but not discontinuously) repulsive core and a weak narrow attractive well centered at about 1.05 core diameters. Marcus and Rice obtained direct evidence for the existence of a hexatic phase that was stable for a substantial range of density, and they observed that the solid-to-hexatic and the hexatic-to-liquid transitions were both first order. Subsequent numerical simu-

lations of a model quasi-2D system designed to mimic that studied by Marcus and Rice, reported by Zangi and Rice [16], reproduce all of the results of the experimental studies. The Zangi-Rice simulations differed from those of Bladon and Frenkel by allowing limited motion of the colloid particles in the direction perpendicular to the plane of the assembly, thereby mimicking the confinement of the colloid particles in a thin cell. In this instance the isostructural solid-solid transition that occurs at high density involves out-of-plane rearrangement of the positions of the colloid particles. The Bladon-Frenkel simulations also lead to the prediction that, when the potential well outside the hard sphere becomes extremely narrow (of order 1% of the particle diameter), the hexatic phase is confined to a very small region on the phase diagram around the solid-solid critical point, and melting proceeds through an ordinary first order solid-to-liquid transition. Experimental evidence supporting this prediction has been furnished by Karnchanaphanurach, Lin, and Rice [14], who studied the melting transition in a quasi-2D assembly of uncharged silica spheres that were stabilized with extremely short chain brushes.

Simulation studies of 2D melting have been carried out for systems with a variety of pair interactions that have, on the scale of the Bladon-Frenkel type interaction, relatively long range. The results of these studies confirm several of the predictions of the KTHNY theory, e.g., the value of the theory specific combination of elastic constants is usually found to be close to the universal value 16π at the melting point (see Ref. [11] and references therein), but there is still not a consensus on such important issues as the dependence of the domain of stability of the hexatic phase and of the character of the melting transition on the form of the pair potential. The literature on this subject is plentiful (for further details we refer the reader to excellent reviews by Strandburg [17] and by Glaser and Clark [11]), so to illustrate this point it suffices to briefly consider only the current situation as regards 2D melting in a system of hard disks. After carrying out a very careful finite-size scaling analysis of the results of Monte Carlo (MC) simulations of a 2D assembly of 16 384 hard disks derived using the innovative subblock method, Weber, Marx, and Binder [18] strongly advocated against the KTHNY melting scenario in favor of a one-stage first order melting process. However, the authors also noted that the observed size dependence of the variation of the fourth order cumulant of the global bond-orientational order parameter with particle density, a measure that is believed to be a sensitive indicator of the order of the underlying phase change, admits the possibility of a single second order melting transition; the prospect of this unconventional melting scenario in 2D has likewise been voiced in the work of Fernandez, Alonso, and Stankiewicz [19]. Nevertheless, Weber, Marx, and Binder have inferred that in their work the cumulative weight of the evidence clearly points to a first order transition as the most probable mechanism for 2D melting in a system of hard disks. These findings have been challenged in a recent study reported by Jaster [20], who carried out Monte Carlo simulations of the properties of hard-disk systems of variable size (up to 65 536 particles), from which he concludes that melting either complies with the KTHNY prediction or, at most, is a weak first order transition. For the case that the pair interaction is continuous but strongly repulsive, notably r^{-12}, Bagchi, Andersen, and Swope [21] have established the dominance of the KTHNY melting mechanism over a conventional first order melting mechanism. They also find that the density range over which the hexatic phase is stable is extremely small, amounting to only 1.2% of the melting density.

Simulations of the mechanism of 2D melting in systems with long range pair interactions also have generated controversial results. Terao and Nakayama [22] have simulated the behavior of a quasi-2D assembly of charged colloidal particles at an air-water interface. The results obtained in these studies favor the KTHNY prediction of two-stage melting with continuous phase transitions. The results of early simulations [23], which were designed to model the behavior of a two-dimensional classical electron system, were interpreted to yield a first order melting transition. However, the latest molecular dynamics studies of Muto and Aoki [24] have suggested that the hexatic phase may, in fact, intervene between the stable solid and liquid phases. While this latter inference seems to agree with the KTHNY prediction, no definitive statement concerning the order of the observed transitions was put forward in this work. The case when the particle-particle interaction is long ranged has also been examined experimentally in a recently reported study of a quasi-2D assembly of colloid particles with magnetic dipole interactions by Zahn, Lenke, and Maret [25]; this study confirms the predictions of the KTHNY theory with respect to melting of the system.

We close these introductory remarks by noting an important finding of Celestini, Ercolessi, and Tosatti [26] that is potentially relevant for the system we study. These investigators have reported the results of molecular dynamics simulations of the structural reconstruction that occurs in the liquid-vapor interface of Au as it is subjected to deep supercooling. They infer that the structure of the liquid-vapor interface of Au is hexatic or, more precisely, that the structure of the interface exhibits extended bond-orientational correlations, and that this hexatic phase persists even when the temperature is 350 °C below the freezing point.

III. SIMULATION DETAILS

A. Potential energy functional

We have studied the properties of a quasi-2D array of Pb atoms as a function of temperature at fixed density. The effective interaction potential between any pair of lead ions was constructed using pseudopotential theory. We remind the reader that the essence of any pseudopotential theory [27–32] lies in the replacement of the strong direct interaction between the delocalized electrons and the ions by an effective, small in magnitude and, in principle, nonlocal pseudopotential that accounts for the requirement that the states of the delocalized electrons are orthogonal to the states of the ion core electrons. The potential part of the Hamiltonian of any arbitrary configuration of N metallic ions and NZ sp valence electrons is then partitioned into two parts. The first part of the pseudopotential representation of the

system energy, the so-called structure independent energy, does not have an explicit dependence on the positions of particles; it depends only on the overall electron density profile. The second part represents the interaction between two metallic pseudoatoms and can be written as

$$V_{\mathrm{eff}}(R;n_{\mathrm{el}}^{\mathrm{LDA}})=\frac{Z^2}{R}\left(1-\frac{2}{\pi}\int_0^\infty \frac{F_N(q)\sin(qR)}{q}dq\right). \quad (1)$$

In the above expression, the first term is the direct Coulomb repulsion between ions of charge Z and the second term describes how the ion-ion interaction is mediated by the valence electrons. V_{eff} is a functional of the electron density, determined for any given pair of particles within some approximation [e.g., a local density approximation (LDA)]. In a homogeneous liquid the dependence of the interaction energy on electron density only influences the total cohesive energy, but not the atomic structure. In an inhomogeneous region of a liquid metal, for example the liquid-vapor interface, the variation of the interaction energy with electron density generates forces that do influence the atomic structure. In this study we ignore the variation of the electron density across the lead monolayer and the changes in the magnitude of V_{eff} associated with local in-plane electron density fluctuations. Our choice of the electron density, required as an input to Eq. (1), was guided by the value determined from fully self-consistent MC simulations of the structure of the liquid-vapor interface of a dilute GaPb alloy performed by Zhao and Rice [4], and was set equal to $0.1174\,e/\text{Å}^3$.

In Eq. (1) the key ingredient is the normalized energy-wave-number characteristic $F_N(q)$, which is quadratic in the electron-ion pseudopotential and can be written (for a local pseudopotential) as

$$F_N(q)=\left(-\frac{q^2\Omega}{2\pi Z^2}\right)\frac{\Omega q^2}{8\pi}\left(\frac{1-\epsilon^H(q)}{\tilde{\epsilon}(q)}\right)|\omega_{\mathrm{bare}}(q)|^2, \quad (2)$$

where $\omega_{\mathrm{bare}}(q)$ is the Fourier transform of the bare pseudopotential and $\epsilon^H(q)$ is the static dielectric function of the electron gas calculated in the random phase approximation (no exchange and correlation contribution). The modified dielectric function $\tilde{\epsilon}(q)$, with exchange and correlation included, is related to $\epsilon^H(q)$ by [28]

$$\tilde{\epsilon}(q)=1+[\epsilon^H(q)-1][1-G(q)], \quad (3)$$

where $G(q)$ is the local field corrector [31], for which we adopt the well-known form due to Ichimaru and Utsumi [33].

In the present work we employ the individual local electron-ion pseudopotential (ILP) of Perdew and coworkers [5]. This potential belongs to a family of local pseudopotentials, known as evanescent core (EC) model potentials, that have been designed specifically for use with a second order nonrelativistic perturbation treatment of the interactions in simple metals. By virtue of its construction, the ILP and its derivatives are continuous throughout space (this smoothness ensures better convergence properties in reciprocal space over lattice vectors), and the evanescence of the core repulsion is naturally incorporated in the form described. The real space representation of the evanescent core pseudopotential is given by [5]

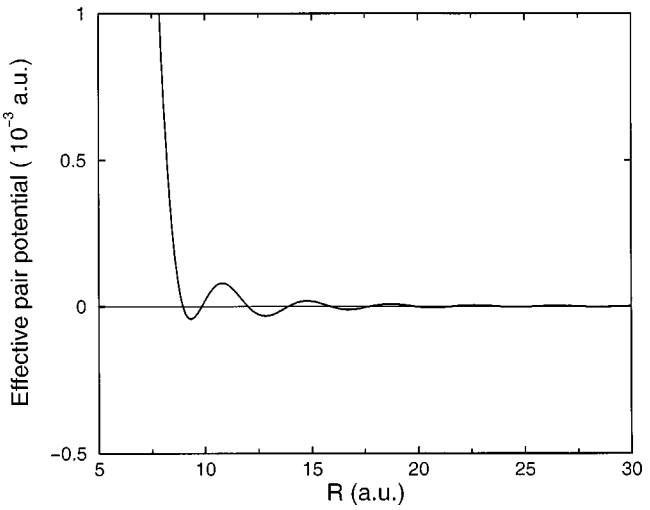

FIG. 1. Effective pair potential for Pb when $\rho_{\mathrm{bulk}}=0.0310$ atoms/Å^3. The axes of this figure are labeled in atomic units for length [1 a.u.$=1a_0$ (Bohr radius)$=0.529\,177$ Å] and energy (1 a.u.$=2$ Ry$=27.21$ eV).

$$\omega_{\mathrm{EC}}(r)=-\frac{Z}{r}\{1-[1+\beta(r/R_{\mathrm{EC}})]\exp(-\alpha r/R_{\mathrm{EC}})\}$$
$$+\frac{Z}{R_{\mathrm{EC}}}A\exp(-r/R_{\mathrm{EC}}), \quad (4)$$

where R_{EC} is the core decay length and $\alpha>0$. Two of the four independent parameters contained in the model, namely, A and β, can be easily determined in terms of α by requiring analyticity of the pseudopotential at $r=0$. The remaining two parameters are fixed by requiring that the total energy per electron of the solid metal, calculated to second order in perturbation theory, is a minimum at the equilibrium value of the Wigner-Seitz radius, and that the valence electron density, calculated to first order in the pseudopotential, is equal for each metal to the value obtained from an all-electron calculation [5]. For Pb we used $R_{\mathrm{EC}}=0.213$ Å and $\alpha=2.950$ with no further parameter adjustment attempted in the course of the simulations. The resultant pair potential is shown in Fig. 1; it has the shape that is typical of pair interactions in simple metals, namely, a steep repulsive core and an algebraically decaying oscillatory tail.

The EC pseudopotentials have been tested extensively for many simple metals. In general, predictions of lattice dynamics, elastic moduli, liquid metal resistivities, binding energies [5,34], and the bulk liquid structure [35,36] are in good agreement with available experimental data. In Fig. 2 we display the very good agreement we have obtained between the calculated and observed pair correlation functions of bulk liquid Pb at two temperatures, one near the melting point and one considerably higher.

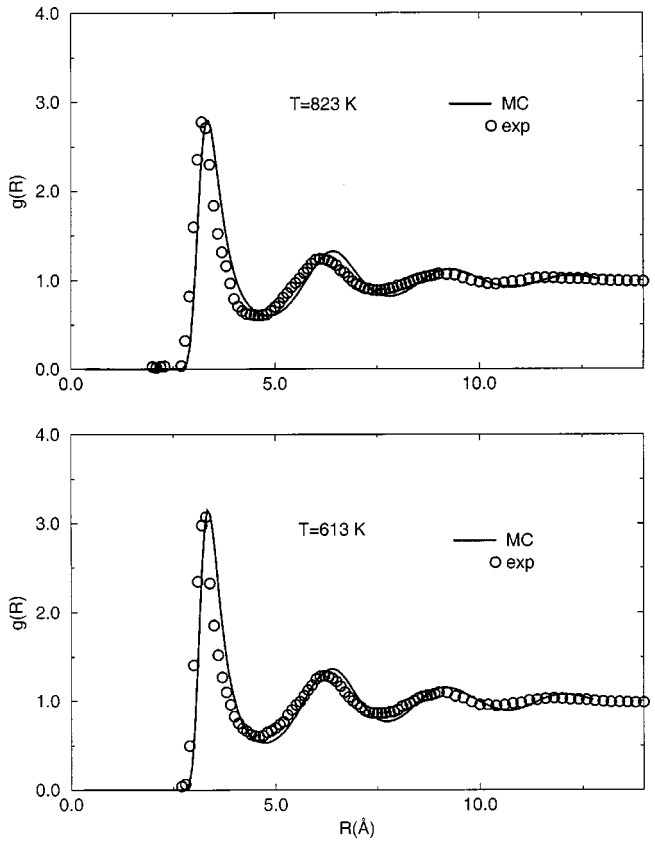

FIG. 2. Comparison of the results of simulations of the pair correlation function of bulk liquid Pb. Lower panel: $T_{expt}=613$ K and $\rho_{bulk}=0.0310$ atoms/Å^3 (——), experiment [41] (○). Upper panel: $T_{expt}=823$ K and $\rho_{bulk}=0.0302$ atoms/Å^3 (——), experiment [41] (○).

B. Computation details

Given the form of the effective pair potential, Monte Carlo simulations were carried out as follows. We placed 2016 Pb pseudoatoms in a rectangular box with side ratio $7:8\sqrt{3}/2$ in the *xy* plane. This sample geometry minimizes the effects due to the boundaries; it can accommodate a perfect 2D triangular crystal with lattice parameter $d=3.42$ Å and, consequently, areal density $\rho_{2D}=0.0987$ atoms/Å^2. The value of d quoted was taken from experiment [1]. The layer thickness was set to 1.5σ, where σ is an effective atomic diameter defined by $\sigma=d$. The out-of-plane (along the *z* direction) particle motion was confined to the range $\pm 0.25\sigma$ around the midplane ($z=0$) by a very steep repulsive potential at the end points. The simulation slab was subject to periodic boundary conditions in the *x* and *y* directions but not in the *z* direction.

The experimental findings of Yang *et al.* [1] suggest only a very small (or zero) change of surface density in the quasi-2D solid-liquid transition of the monolayer of Pb segregated in the liquid-vapor interface of a dilute Pb in Ga alloy. Therefore, in our calculations we fixed ρ_{2D} at the value characteristic of the experimentally observed solid phase and kept it fixed throughout the course of the simulations. With this constraint, the melting process follows a line of constant density in the phase diagram. The system melts as the temperature is gradually raised from a value in the domain of stability of the ordered solid to a value in the domain of stability of the disordered phase.

Before proceeding further we must comment on the magnitude of the out-of-plane motion and the temperatures used in our simulations. As will be seen, the melting temperature of the simulated quasi-two-dimensional Pb layer is found to be much higher than the melting temperature of bulk Pb. We argue that this displacement of the temperature scale from that of the experimental system is primarily an artifact introduced by the restriction placed on the allowed out-of-plane motion motion of the Pb atoms. The value for the allowed out-of-plane motion used in this paper was chosen to mimic the mean layer thickness found in the simulations of the structure of the liquid-vapor interface of a Pb in Ga alloy reported by Zhao and Rice [4]. As is the case with other simulations of the structure of the liquid metal-vapor interface, because the finite size of the simulation sample cannot adequately represent long wavelength fluctuations of the interface, their results overestimate the amplitude of the first peak in the density distribution along the normal, and they underestimate the width of that peak. Moreover, the energy associated with the out-of-plane motion is determined only by the interaction between the Pb atoms in the layer, so that application of the constraint that the amplitude cannot exceed $\pm 0.25\sigma$ from the midplane is equivalent to confining the Pb atoms in a parallelepiped with thickness 1.5σ. In calculations now under way, but not yet complete, the out-of-plane motion of the Pb atoms has been treated differently; this motion is allowed to be arbitrarily large but is constrained by an additional parabolic potential centered at $z=0$. The width of the distribution of out-of-plane motions is taken to be the root-mean-square amplitude determined from the experimental studies. All of the qualitative features of the preliminary results obtained from these latter calculations are the same as those reported later in this paper, but the temperature scale is shifted so that the melting of the layer occurs near 450 instead of near 1250 K. There is also likely to be a contribution to the temperature shift from the shortcomings of the local pseudopotential used in our calculations. It is commonly found that a local pseudopotential representation of the interaction between atoms in a bulk metal generates an excellent description of the structure of the metal, but a poor representation of the binding energy. For this reason, a local pseudopotential is often semiempirically modified to remove the discrepancy between the calculated and observed binding energy and the system pressure [32,36]. As shown in Fig. 2, the local pseudopotential we have used does generate a bulk liquid Pb pair correlation function that is in very good agreement with the observed pair correlation function at $T=613$ and 823 K, and it does so without the use of semiempirical modifications. However, the energy difference between the bulk liquid and solid phases is less accurately reproduced. From the evidence available from the general character of calculations that use the pseudopotential representation, we believe that all of the qualitative features of the quasi-2D melting transition, specifically those associated with the structures involved, are preserved despite the shift in temperature scale associated with the amplitude of out-of-

plane motion and the local pseudopotential we have employed.

The simulations were started by placing the pseudoatoms at the sites of a perfect 2D triangular lattice located in the plane defined by $z=0$. As the system evolves, particles tend to stray away from the midplane, filling up the layer volume. In the course of a simulation ions are moved sequentially, one at a time, and the new configurations are accepted or rejected according to the standard Metropolis procedure [37] by consulting the appropriate Boltzmann factors. A large number of MC steps (in a MC step we attempt to move each particle once) is required for a system to reach equilibrium. Prior to collecting the final statistics for analysis, the low-temperature simulations (between 300 and 1100 K) were carried out for about $(500\times10^3)-(750\times10^3)$ steps, whereas the high-T simulations (from 1700 to 2000 K) were run for about 400×10^3 steps. As an additional indicator of our ability to successfully equilibrate the system we remark on the results of the following test. At 2000 K, two distinct simulation routes were explored, one with an initial configuration with the particles placed randomly in the midplane (but removing configurations with core-core overlap), the other with particles placed on a 2D hexagonal lattice. After about 150×10^3MC steps these systems became physically indistinguishable, thereby providing an estimate for the lower bound of the number of MC steps needed for equilibration of our system.

Special care was taken in equilibrating the model system in the temperature range between 1200 and 1600 K. In this temperature domain the defect structure of the underlying particle configurations is usually quite complex, so that a lengthy equilibration period is needed, which in our study was about 950×10^3MC steps.

For each temperature, the approach to equilibrium was checked by monitoring, in successive simulation runs, the decrease of the energy and the changes in the structural correlation functions. Following achievement of equilibrium, averages were calculated from the data collected every 50 MC steps from additional MC runs of about 50×10^3 to 100×10^3 steps.

To monitor the structural change occurring in the melting process, we elected to work with two sets of order parameters. One set consists of the global bond-orientational and global translational order parameters, denoted GOOP and GTOP, respectively. These quantities provide information on the overall character of the melting process. We have also calculated the local bond-orientational order parameter, which measures the (average) orientational symmetry immediately around a pseudoatom.

Adhering to the widely used convention, for each particle we define [9,11]

$$\psi_{6i}=\frac{1}{n_i}\sum_{j=1}^{n_i} e^{i6\theta(R_{ij})}, \tag{5}$$

where n_i is the number of nearest neighbors (NN's) of the ith particle and $\theta(R_{ij})$ designates the angle between the imaginary bond R_{ij} connecting particles i and j and an arbitrary axis x. The NN list was compiled for each pseudoatom in a chosen configuration from the associated Voronoi polygon mapping of that configuration [38]. The local bond-orientational order parameter is computed from

$$|\psi_{6i}|^2=\frac{1}{n_i}\sum_{j=1}^{n_i}\psi_{6j}^{*}\psi_{6i}. \tag{6}$$

For a perfect 2D hexagonal solid, $|\psi_{6i}|^2=1$. In contrast, for a disordered system the peak of the distribution of $|\psi_{6i}|^2$ is shifted toward zero, signaling the loss of the orientational symmetry in the first neighbor shell of a pseudoatom.

The global bond-orientational order parameter is defined by

$$\Psi_6=\frac{1}{N}\sum_{i=1}^{N}\psi_{6i}, \tag{7}$$

where summation extends over all N pseudoatoms in the box. Similarly, the global translational order parameter is defined by

$$\Psi_T=\frac{1}{N}\sum_{i=1}^{N} e^{i\mathbf{G}\cdot\mathbf{R}_i}. \tag{8}$$

In Eq. (8), $\mathbf{G}$ denotes a reciprocal lattice vector of the triangular lattice and $\mathbf{R}_i$ is the position vector of the ith particle. A crude method for identifying the thermodynamically stable phases that participate in the process of melting of a quasi-2D metallic system can be based on considering the magnitudes of the calculated values of the GOOP and GTOP. For a disordered liquid phase these values must be much less than unity. In contrast, in a typical 2D solid one finds that $0<|\Psi_6|$, $|\Psi_T|<1$, with these values rapidly approaching unity as the structure becomes progressively more ordered and more defect-free. More insight can be gained from an analysis of the correlation lengths associated with the GOOP and GTOP. This information can be extracted from the decays of the envelopes of the corresponding correlation functions, namely, the orientation correlation function [9,11,16,17]

$$g_6(R)=\langle\psi_6^{*}(0)\psi_6(R)\rangle \tag{9}$$

and the pair correlation function [39]

$$g(R)=\frac{V}{N^2}\left\langle 2\sum_{i=1}^{N}\sum_{j<i}^{N}\delta(\mathbf{R}-\mathbf{R}_{ij})\right\rangle, \tag{10}$$

where $\langle\cdots\rangle$ refers to an ensemble average. In the above expressions, the vectors and distances in the arguments are the projections of the 3D quantities onto the xy plane.

Additional information concerning the nature of a phase can be obtained from an analysis of the diffraction pattern associated with the particle configuration in that phase. We have computed both the 2D static structure factor $S(\mathbf{q}_{xy})$ and the angle-averaged static structure factor $S(q_{xy})$. The structure factor is defined by

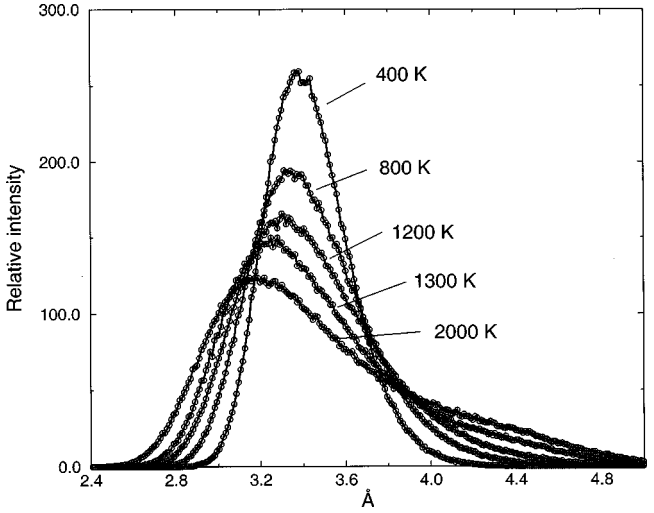

FIG. 3. Nearest-neighbor bond length distribution functions computed for several temperatures. The low-temperature lattice spacing is 3.42 Å.

$$S(\mathbf{q}_{xy}) = \frac{1}{N}\left\langle \sum_{n=1}^{N} e^{i\mathbf{q}_{xy}\cdot\mathbf{x}_n} \sum_{m=1}^{N} e^{-i\mathbf{q}_{xy}\cdot\mathbf{x}_m} \right\rangle, \qquad (11)$$

where $\mathbf{q}_{xy}$ is a 2D wave vector and $\mathbf{x}_n$ and $\mathbf{x}_m$ are 2D projections of the position vectors of particles n and m onto the xy plane. When averaged over angles, the above expression reduces to

$$S(q_{xy}) = 1 + \frac{2}{N}\left\langle \sum_{r_{nm}} J_0(q_{xy} r_{nm}) \right\rangle. \qquad (12)$$

In Eq. (12), J_0 designates the zeroth order regular Bessel function and the sum runs over all distinct pairs of particles. Due to the small size of the simulation sample, we cannot use Eq. (12) to capture the correct long wavelength behavior of the structure factor. Numerically, this would inevitably result in spurious fluctuations of $S(q_{xy})$ in the small q domain. Still, for the simulation samples we have studied, we found that the positions and magnitudes of the first several peaks in $S(q_{xy})$ can be established with confidence.

IV. RESULTS AND DISCUSSION

We now examine the results of our calculations. Figure 3 shows the nearest-neighbor separation distribution functions in the quasi-2D Pb array, computed for particle configurations at several different temperatures. These distributions are unimodal at all temperatures, and they clearly show that the most probable nearest-neighbor separation moves to smaller values as the temperature increases. The decrease of the average nearest-neighbor separation with increasing temperature is the behavior expected for a system with pair potential of the form displayed in Fig. 1.

Figure 4 displays the distribution of the local bond-orientational order parameter as a function of temperature. The behavior of this order parameter is consistent with the occurrence of a phase transition, and the bimodal shape of some of the intermediate distributions is consistent with that

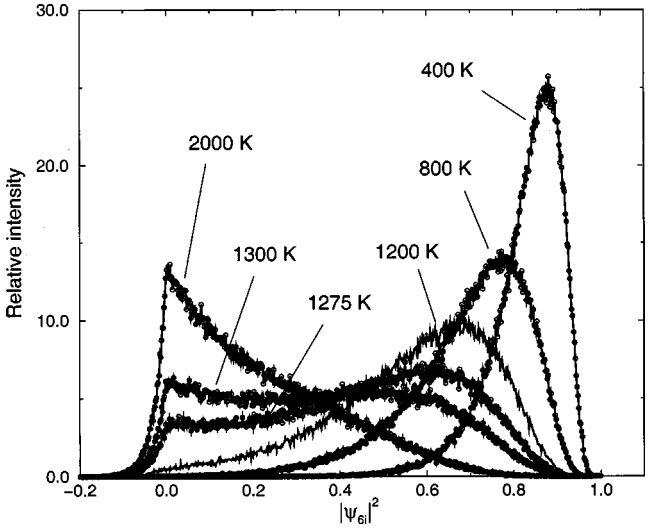

FIG. 4. The local bond-orientation order parameter distribution functions as a function of temperature.

transition being first order. However, the bimodal structure of the distribution of $|\psi_{6i}|^2$ is not a completely unambiguous signature of phase coexistence and hence of a first order transition. The order of a phase transition can best be inferred from a study of the size dependence of the distribution of $|\psi_{6i}|^2$ [20].

The dependences of the global order parameters on temperature are displayed in Fig. 5. For $T<1250$ K both parameters decrease almost linearly with temperature, albeit with slightly different slopes. For $T>1275$ K the translational order parameter is very small, and for $T>1500$ K the bond-orientation order parameter is very small. We will discuss the behavior of the system in the temperature range $1275 < T < 1500$ K later in this paper. Note that the sharp decrease in the value of the global bond-orientation order parameter occurs at a higher temperature than does the corresponding

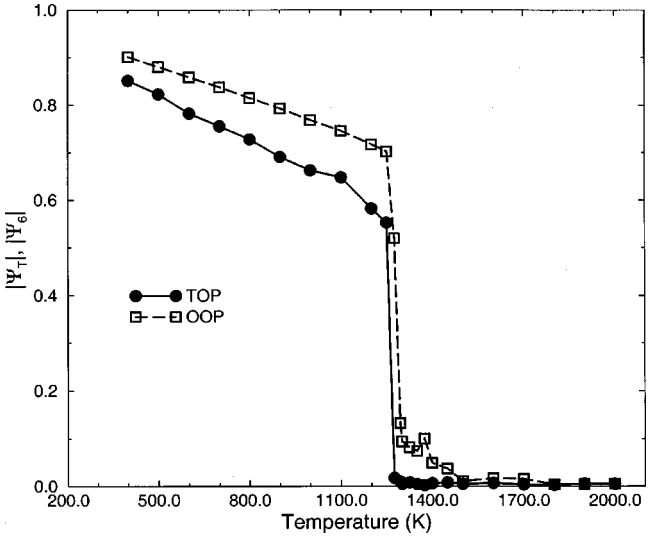

FIG. 5. The magnitude of the global translational (●) and bond-orientation (□) order parameters as a function of temperature. Lines are guides to the eye.

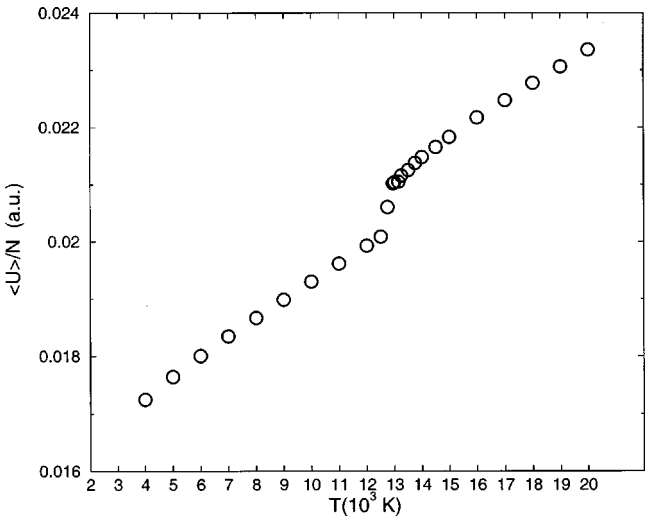

FIG. 6. Average potential energy per particle as a function of temperature. For energy units refer to the caption to Fig. 1.

sharp decrease in the value of the translational order parameter. These data suggest that there is a small temperature range in which there is a stable phase with persistent bond-orientation order but very short ranged translational order, i.e., a hexatic phase. Our simulation data suggest that when $\rho_{2D}=0.0987$ atoms/Å^2, for the pseudopotential used, the hexatic phase is stable in the temperature range $1250<T<1295$ K.

We display in Fig. 6 the average value of the potential energy per particle. In agreement with previously reported studies [40], the potential energies of the solid and liquid phases are (almost) linear functions of the temperature, respectively, below and above the transition. There is a very clear dramatic increase in the potential energy per pseudoatom in the temperature range between 1250 and 1295 K, consistent with the occurrence of a first order transition. Assuming that the observed transition is, in fact, first order, we can easily estimate the entropy change per pseudoatom associated with melting. Imposing the condition for phase equilibrium $\Delta\mu=\Delta\varepsilon-T\Delta s+p\Delta v=0$, assuming that the kinetic energy scales linearly with temperature, and remembering that in our system $\Delta v=0$, yields $\Delta s\sim 0.21k_B$ at $T=1250$ K. This value for the entropy change on melting is somewhat smaller than the generally accepted value of $0.3k_B$ found for 2D systems with long range potentials [11].

An independent means of substantiating the proposition that the melting of the quasi-2D Pb monolayer is a first order transition is to study the freezing process while monitoring the same functions as in the study of the melting process. We have carried out a few simulations of this type. The preliminary results obtained suggest that there is hysteresis in the temperature dependence of the potential energy, an observation that supports the suggestion that the melting process is first order. However, we do not take these preliminary results to be definitive because, within the computation time available, we were unable to fully equilibrate configurations at 1100, 1200, and 1300 K. For these particular configurations the densities of defects were found to be higher than for their counterparts examined in the melting sequence, exemplifying the very slow relaxation of defects commonly observed in canonical ensemble simulations [17].

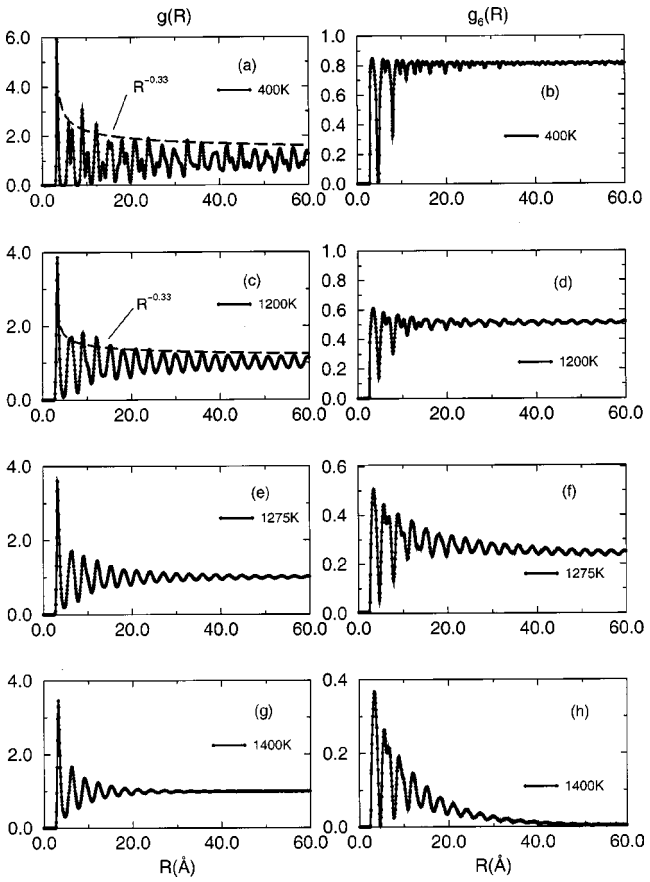

FIG. 7. Pair correlation and bond-orientation correlation functions computed at 400 (a) and (b), 1200 (c) and (d), 1275 (e) and (f), and 1400 K (g) and (h). The dashed lines shown in (a) and (c) represent power law fits to the simulation data.

Identification of the hexatic phase relies on the observation of the simultaneous existence of quasi-long-range bond-orientational order and short range translational order. Although the size of our simulation sample limits the accuracy with which we can determine the decay of the envelopes of $g_6(R)$ and $g(R)$, we have carried out those determinations. Figure 7 displays $g_6(R)$ and $g(R)$ for a few thermodynamic states. For $T=400$ and 1200 K, the envelope of $g(R)$ decays algebraically with exponent $\eta_T\sim\frac{1}{3}$ and the envelope of $g_6(R)$ does not decay (see Fig. 8), as predicted by the KTHNY theory. For $T=1300$ and 1400 K the envelopes of $g_6(R)$ and $g(R)$ decay exponentially (see Fig. 8), as expected. However, when $T=1275$ K, which is just inside the region that we identify with a stable hexatic phase, the envelope of $g_6(R)$ displays algebraic decay with $\eta_6=0.13$, consistent with the KTHNY prediction for the hexatic phase $0<\eta_6<0.25$. To complement these observations we have computed the diffraction patterns and angle-averaged static structure factors for several thermodynamic states spanning the temperature region from solid to liquid. Some of the results are shown in Fig. 9. The low-temperature (400 K) diffraction pattern, which agrees very well with that observed below the melting transition, has sharp Bragg peaks

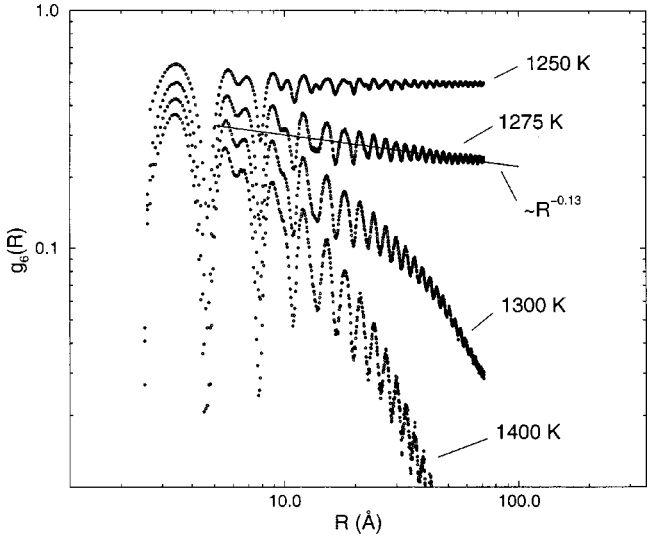

FIG. 8. Bond-orientation correlation functions computed at $T=1250$, 1275, 1300, and 1400 K. The linear fit shown corresponds to an algebraic decay of the envelope as $R^{-0.13}$.

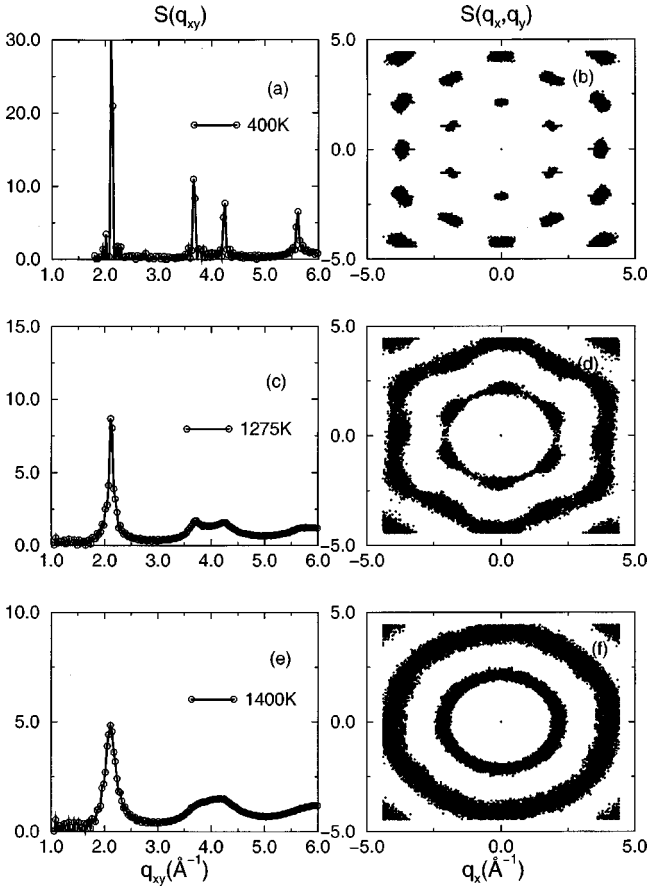

FIG. 9. Angle-averaged static structure functions and the corresponding diffraction patterns at $T=400$ (a) and (b), 1275 (c) and (d), and 1400 K (e) and (f). In each case the small q_{xy} domain of $S(q_{xy})$ has been omitted (see text discussion). Lines are guides to the eye.

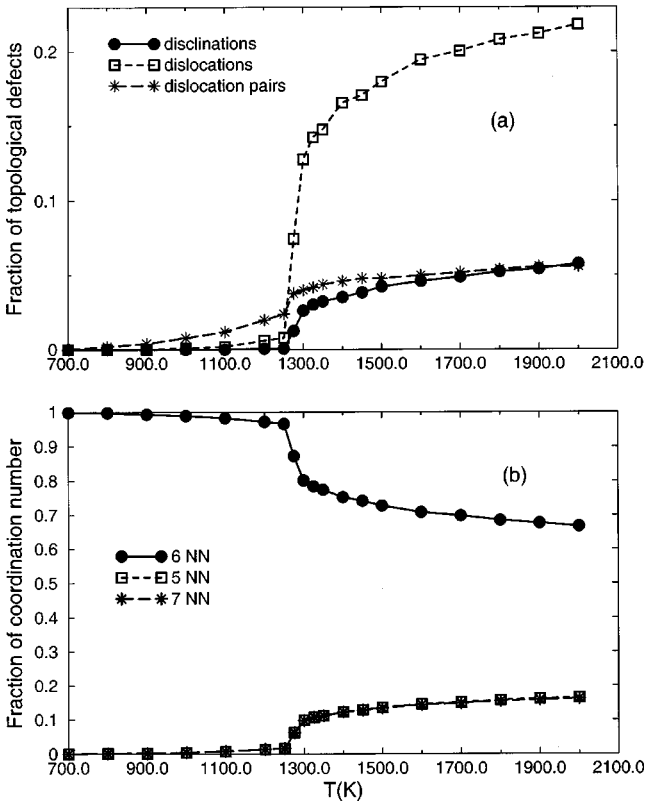

FIG. 10. (a) Fraction of disclinations (●), dislocations (□), and dislocation pairs (∗) as a function of temperature. (b) Fraction of pseudoatoms that have six (●), five (□), and seven nearest neighbors (∗) as a function of temperature. Lines are guides to the eye.

characteristic of a hexagonal lattice; it is consistent with the existence of hexagonal packing in the Pb monolayer. The diffraction patterns of the equilibrium phases generated in our simulations retain this character at all temperatures up to $T=1250$ K. The 1275 K diffraction pattern is very similar to that observed just above the melting transition [1], which suggests that the Pb monolayer segregated in the liquid-vapor interface of a dilute Pb in Ga alloy melts from a hexagonal solid to a hexatic phase. At 1400 K, the concentric ring structure of the diffraction pattern is a reliable indicator that the system has become a liquid, again in agreement with the observed diffraction pattern when the temperature is 20 K greater than that of the hexagonal solid-to-hexatic transition [2]. Indeed, the variation of the shape of $S(q_{xy})$ with temperature in our simulation data follows precisely the same trend as found experimentally [1]. The positions of the first few peaks in the angle-averaged structure factor remain virtually unchanged as the system is transformed from solid to liquid.

We consider now the character and distribution of defects as the solid-to-liquid phase transition is traversed. We have followed the conventional procedure of identifying defects via the Voronoi polygon mapping of the pseudoatom spatial configuration. A defect is defined to be a pseudoatom with other than six nearest neighbors; these are mapped as Voronoi polygons with other than six sides. There are sev-

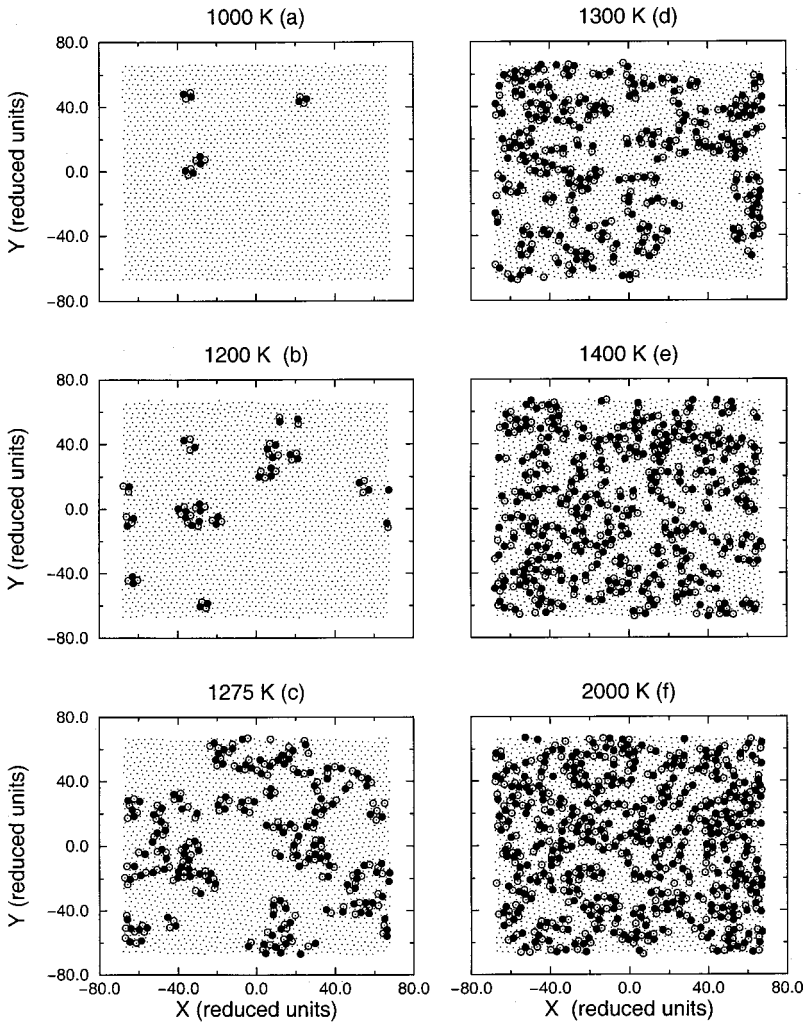

FIG. 11. Snapshots of equilibrium pseudoatom configurations at 1000 (a), 1200 (b), 1275 (c), 1300 (d), 1400 (e), and 2000 K (f). Open circles mark five fold coordinated pseudoatoms, filled circles sevenfold coordinated pseudoatoms.

eral kinds of defects. Sevenfold and fivefold Voronoi polygons are classified as free disclinations [9]. A bound pair of sevenfold and fivefold defects is a dislocation. At any nonzero temperature the 2D solid has a small concentration of bound pairs of dislocations (quartets of disclinations) but their presence does not disrupt the quasi-long-range translational order. At any given temperature in the stable domain of the 2D solid, defects with different coordination numbers, say 4 and 8, have significantly smaller concentrations than the defects already mentioned. Consequently, they are assumed to play a minor role in defining the melting process. The concentrations of dislocation pairs, dislocations, and disclinations in our simulation sample, as a function of temperature, are shown in Fig. 10, and snapshots of several defect distributions are shown in Fig. 11. Well below the melting temperature, the defect structure of the 2D solid is consistent with the assumptions of the KTHNY theory. In this temperature regime defects occur only in the form of tightly bound dislocation pairs and are present at very small concentrations ($<2\%$). At about 1100 K, isolated dislocations start to appear, but dislocation pairs are still the dominant defects. This situation persists up to 1250 K. We also note that up to 1250 K there is a vanishingly small concentration of free disclinations, in agreement with the KTHNY prediction. The evident clustering of defects in the 1275 K image [see Fig. 11(c)] implies that the newly formed dislocations are not independent entities. The short, curved, chainlike arrangements of dislocations grow rapidly to produce a highly branched network of defects at 1400 K [Fig. 11(e)], at which temperature the system is a 2D liquid. The observed evolution of the intrinsic defect structure is, in principle, compatible with those theories that assert that 2D melting occurs via the formation, interaction, and propagation of collective excitations of defects. Such theories usually predict that the 2D melting transition is first order.

Finally, we wish to address briefly the somewhat surprising behavior of the global bond-orientation order parameter in the temperature range between 1300 and 1500 K (Fig. 5). As evident from the preceding discussion, for $T \gtrsim 1300$ K the quasi-2D metallic system behaves essentially as a liquid. However, for $1295 < T < 1500$ K Ψ_6 exhibits values small in magnitude but nevertheless substantially higher than the corresponding values of the global translational order parameter Ψ_T. Although no direct verification has been attempted in the current study, it seems plausible that such inconsistency is a size related effect, especially given the fact that for a quasi-2D disordered system the range of correlations between the orientations of virtual bonds may be longer than the correlation lengths associated with translational symme-

try. Similar Ψ_6 vs T dependence has been reported by Zangi and Rice in a MD study of a quasi-2D model colloidal system (see Fig. 7 of Ref. [16]), but, despite the fundamental difference in the forms of the particle interaction potential used in that study and in our calculations, both sets of simulations were conducted in almost identical sample geometries. For a system of a considerably larger size, we then expect the ''toe'' region of the Ψ_6 vs T diagram to flatten, making the second, hexatic-to-liquid, transition look more like a first order transition.

ACKNOWLEDGMENTS

We wish to thank Dr. Ronen Zangi for his assistance with program codes and numerous valuable discussions. This work was supported by the National Science Foundation (Grant No. CHE-9800071).

[1] B. Yang, D. Gidalevitz, D. Li, Z. Huang, and S. A. Rice, Proc. Natl. Acad. Sci. U.S.A. **96**, 13 009 (1999).
[2] B. Yang, D. Li, Z. Huang, and S. A. Rice, Phys. Rev. B **62**, 13 111 (2000).
[3] M. Zhao, D. Chekmarev, and S. A. Rice, J. Chem. Phys. **108**, 5055 (1998); S. A. Rice and M. Zhao, Phys. Rev. B **57**, 13 501 (1998); M. Zhao and S. A. Rice, J. Chem. Phys. **111**, 2181 (1999).
[4] M. Zhao and S. A. Rice, Phys. Rev. B (to be published).
[5] C. Fiolhais, J. P. Perdew, S. Q. Armster, J. M. MacLaren, and M. Brajczewska, Phys. Rev. B **51**, 14 001 (1995).
[6] R. Peierls, Ann. Inst. Henri Poincare **5**, 177 (1935); L. D. Landau, Phys. Z. Sowjetunion **11**, 26 (1937); L. D. Landau and E. M. Lifshits, *Statistical Physics* (Pergamon, Oxford, 1986); N. D. Mermin, Phys. Rev. **176**, 250 (1968).
[7] B. Krishnamachari and G. V. Chester, Phys. Rev. B **61**, 9677 (2000).
[8] J. M. Kosterlitz and D. J. Thouless, J. Phys. C **5**, L124 (1972); **6**, 1181 (1973); B. I. Halperin and D. R. Nelson, Phys. Rev. Lett. **41**, 121 (1978); D. R. Nelson and B. I. Halperin, Phys. Rev. B **19**, 2457 (1979); A. P. Young, *ibid.* **19**, 1855 (1979).
[9] D. R. Nelson, in *Phase Transitions and Critical Phenomena*, edited by C. Domb and J. L. Lebowitz (Academic, London, 1983), Vol. 7.
[10] S. T. Chui, Phys. Rev. B **28**, 178 (1983).
[11] M. A. Glaser and N. A. Clark, Adv. Chem. Phys. **83**, 543 (1993).
[12] C. A. Murray and D. H. Van Winkle, Phys. Rev. Lett. **58**, 1200 (1988); C. A. Murray and R. A. Wenk, *ibid.* **62**, 1643 (1989); C. A. Murray, W. O. Sprenger, and R. A. Wenk, Phys. Rev. B **42**, 688 (1990).
[13] A. H. Marcus and S. A. Rice, Phys. Rev. Lett. **74**, 2519 (1995); Phys. Rev. E **55**, 637 (1997).
[14] P. Karnchanaphanurach, B. H. Lin, and S. A. Rice, Phys. Rev. E **61**, 4036 (2000).
[15] P. Bladon and D. Frenkel, Phys. Rev. Lett. **74**, 2519 (1995).
[16] R. Zangi and S. A. Rice, Phys. Rev. E **58**, 7529 (1998).
[17] K. J. Strandburg, Rev. Mod. Phys. **60**, 161 (1988).
[18] H. Weber, D. Marx, and K. Binder, Phys. Rev. B **51**, 14 636 (1995).
[19] J. F. Fernandez, J. J. Alonso, and J. Stankiewicz, Phys. Rev. Lett. **75**, 3477 (1995); H. Weber and D. Marx, *ibid.* **78**, 398 (1997); J. F. Fernandez, J. J. Alonso, and J. Stankiewicz, *ibid.* **78**, 399 (1997).
[20] A. Jaster, Phys. Rev. E **59**, 2594 (1999).
[21] K. Bagchi, H. C. Andersen, and W. Swope, Phys. Rev. Lett. **76**, 255 (1996).
[22] T. Terao and T. Nakayama, Phys. Rev. E **60**, 7157 (1999).
[23] R. K. Kalia, P. Vashishta, and S. W. de Leeuw, Phys. Rev. B **23**, 4794 (1981).
[24] S. Muto and H. Aoki, Phys. Rev. B **59**, 14 911 (1999); Physica E **6**, 116 (2000).
[25] K. Zahn, R. Lenke, and G. Maret, Phys. Rev. Lett. **82**, 2721 (1999).
[26] F. Celestini, F. Ercolessi, and E. Tosatti, Phys. Rev. Lett. **78**, 3153 (1997).
[27] M. Zhao, D. Chekmarev, Z. Cai, and S. A. Rice, Phys. Rev. E **56**, 7033 (1997).
[28] M. P. D'Evelyn and S. A. Rice, J. Chem. Phys. **78**, 5225 (1983).
[29] J. G. Harris, J. Gryko, and S. A. Rice, J. Chem. Phys. **87**, 3069 (1987).
[30] W. A. Harrison, *Pseudopotentials in the Theory of Metals* (Benjamin, New York, 1966).
[31] J. Hafner, *From Hamiltonians to Phase Diagrams* (Springer-Verlag, Berlin, 1987).
[32] D. Chekmarev, M. Zhao, and S. A. Rice, J. Chem. Phys. **109**, 768 (1998).
[33] S. Ichimaru and K. Utsumi, Phys. Rev. B **24**, 7385 (1981).
[34] L. Pollack, J. P. Perdew, J. He, M. Marques, F. Nogueira, and C. Fiolhais, Phys. Rev. B **55**, 15 544 (1997).
[35] M. Boulahbak, N. Jakse, J.-F. Wax, and J.-L. Bretonnet, J. Chem. Phys. **108**, 2111 (1998).
[36] D. S. Chekmarev, D. W. Oxtoby, and S. A. Rice, Phys. Rev. B **61**, 10 116 (2000).
[37] N. Metropolis, A. W. Rosenbluth, M. N. Rosenbluth, A. M. Teller, and E. Teller, J. Chem. Phys. **21**, 1087 (1953).
[38] J. O'Rourke, *Computational Geometry in C* (Cambridge University Press, London, 1998).
[39] M. P. Allen and D. J. Tildesley, *Computer Simulation of Liquids* (Clarendon, Oxford, 1989).
[40] I. V. Schweigert, V. A. Schweigert, and F. M. Peeters, Phys. Rev. B **60**, 14 665 (1999).
[41] Y. Waseda, *The Structure of Non-Crystalline Materials—Liquids and Amorphous Solids* (McGraw-Hill, New York, 1980).